Chemical Engineering Journal 160 (2010) 760–769

Contents lists available at ScienceDirect

Chemical Engineering Journal

journal homepage: www.elsevier.com/locate/cej

Synergies in the production of olefins by combined cracking of n-butane and methanol on a HZSM-5 zeolite catalyst

Diana Mier*, Andres T. Aguayo, Ana G. Gayubo, Martin Olazar, Javier Bilbao

Departamento de Ingeniería Química, Universidad del País Vasco, Apartado 644, 48080 Bilbao, Spain

ARTICLE INFO

Article history:
Received 4 February 2010
Received in revised form 7 April 2010
Accepted 8 April 2010

Keywords:
n-Butane cracking
Olefins
Methanol
HZSM-5 zeolite
Process integration
Coke
Deactivation

ABSTRACT

The production of olefins by the joint transformation of n-butane and methanol has been studied in a fixed bed reactor on a HZSM-5 zeolite catalyst in the 400–575 °C temperature range. A methanol/n-butane molar ratio of 3 has been used in order to obtain an energy-neutral integrated process, which enhances the activity in the cracking reaction. Moreover, the joint transformation of the two reactants generates a reaction medium with favourable composition for improving the yield and selectivity of C_2–C_4 olefins compared to the two individual reactions. The olefins formed in n-butane cracking play a significant role for both activating the methanol transformation mechanism and attenuating coke formation. Likewise, the water formed in methanol dehydration also plays a significant role for attenuating the hydrogen transfer reactions in n-butane cracking. These synergistic effects contribute to increasing olefin yields for low values of space time, which has been quantified by means of a coefficient.

1. Introduction

The petrochemical industry needs to respond quickly to market requirements by increasing the production of raw materials with growing demand, such as olefins and especially propylene. Fig. 1 schematically shows the processes for olefin production from different raw materials, which have been ordered according to their contribution to sustainability.

The forecast for raw material availability is 40 years for oil, 70 years for natural gas and 170 years for coal, which are estimations based on the current consumption rate and excluding the reserves of oil sands and shales [1,2]. In this context, the challenge facing the petrochemical industry is to promote the upgrading of natural gas and coal and progressively valorise biomass products, especially lignocellulosic ones, thus contributing to a reduction in CO_2 emissions [3–5].

The main sources of C_2–C_4 olefins are the following units: steam cracking (70%), catalytic cracking (FCC) (fluidized catalytic cracking) (18%) and the MTO process (methanol to olefins) (10%), whereas the remaining 2% is obtained by paraffin dehydrogenation (and oxidative dehydrogenation) and by metathesis [6]. This imbalance in favour of steam cracking and FCC units for olefin production is likely to persist over the coming years, given that important progress is being made in these units in pursuit of this objective, whereas the industrial implementation of alternative processes is not imminent [7,8].

In the steam cracking process, the nature of the feed plays an essential role in selectivity, so that 25% of ethylene is obtained with a HVGO (heavy vacuum gas oil), whereas when feeding ethane (separated from natural gas, in which its content is about 4%), the yield is increased to 80% and coke production in the unit is minimized [7].

Large-scale catalytic cracking (FCC) units are becoming more important in olefin production due to the modifications in the catalyst (with HZSM-5 as additive) and to the recirculation and overcracking of stream products [9,10]. Thus, naphtha recirculation can provide a selectivity of C_2–C_4 olefins of up to 70%, with 35% propylene selectivity, although with a low conversion [11]. Wang et al. [12] have proposed an additional reactor (riser) for naphtha overcracking, which allows achieving (at pilot plant scale) a conversion of 47% with propylene selectivity of 39%. Moreover, olefin production in FCC units can be increased by valorising streams from other units in the refinery, such as the waxes from FT (Fischer–Tropsch) synthesis [13], heavy naphthas from the coker and visbreaker units [14,15], and the atmospheric distillation residue [16]. The most significant innovations developed in a demonstration scale plant (30 barrels/day) by the consortium Nippon-Oil Corporation and Saudi ARAMCO correspond to High-Severity Fluidized Cracking (HS-FCC) [17], with a propylene yield of 25% feeding VGO (vacuum gas oil). There are also encouraging laboratory results concerning olefin production obtained by co-feeding waste plastics [18,19] or waste plastic pyrolysis waxes into FCC units [20].

* Corresponding author. Tel.: +34 94 601 5501.
E-mail address: diana.mier@ehu.es (D. Mier).

1385-8947/$ – see front matter © 2010 Elsevier B.V. All rights reserved.
doi:10.1016/j.cej.2010.04.016

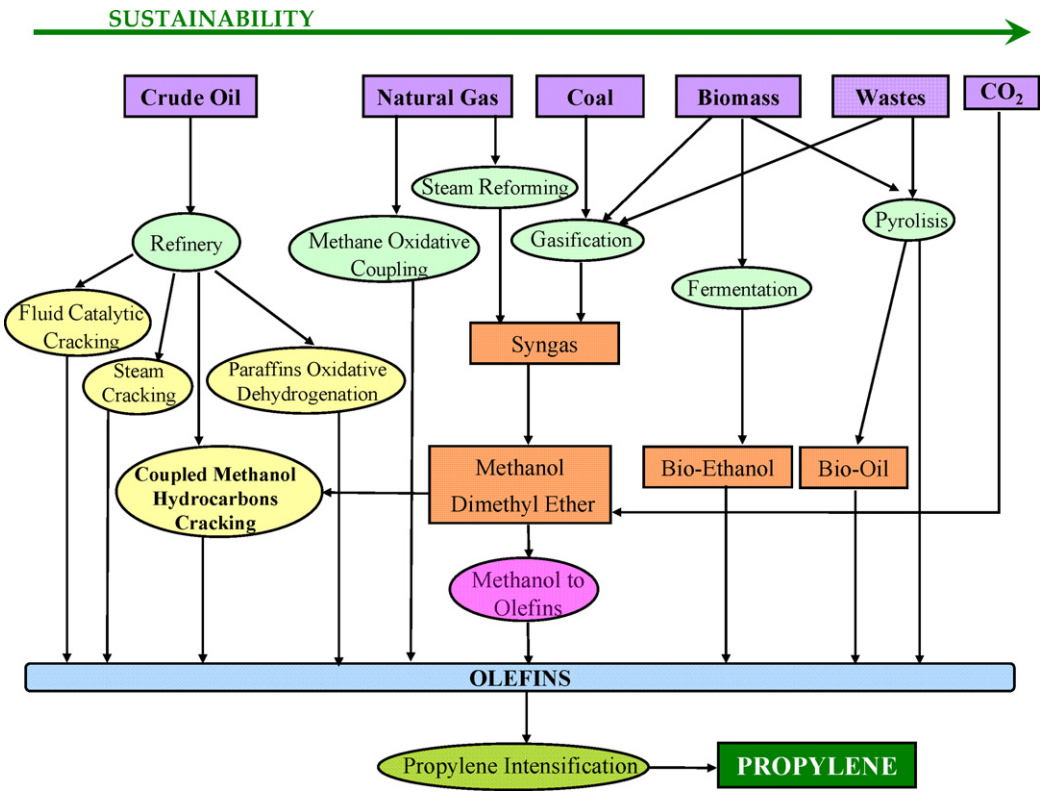

Fig. 1. Processes for olefin production.

Amongst the processes with paraffins as feedstock, dehydrogenation increases propylene selectivity compared to steam cracking. The technological development achieved with propane as feedstock is notable, although given the endothermicity of the dehydrogenation, alternative processes (in fixed or fluidised bed reactors) have the disadvantage of high energy consumption, CO_2 emissions and high coke deposition on the catalyst [21]. The energy requirement is avoided by oxidative dehydrogenation (ODHP) with O_2, which contributes to coke combustion and so attenuates catalyst deactivation. Furthermore, the use of CO_2 is studied as an oxidizer for helping to mitigate the greenhouse effect [22]. The industrial implementation of these processes requires the large-scale development of new catalytic reactors (such as those formed by multi-channel monoliths), which are suitable for the reduced contact times (ms) required for acceptable olefin selectivity [23–25].

Methane valorisation has traditionally aroused great interest, with the aim being to replace oil with natural gas to obtain fuel and feedstock for the petrochemical industry. Unfortunately, methane reactions are thermodynamically unfavoured [26]. The direct oxidative conversion of methane (methane oxidative coupling, MOC) involves difficulties for controlling the exothermicity of the reaction and for increasing the selectivity of olefins by minimizing CO_2 formation [27–29]. As in the aforementioned processes, technological research is focused on improving the catalyst and on developing new reactors. In this case, membrane reactors provide encouraging results (at laboratory scale) [30].

This paper studies the joint catalytic transformation of paraffins (n-butane) and methanol over a HZSM-5 zeolite with the aim of obtaining olefins. Martin et al. [31] proposed the CMHC (coupled methanol–hydrocarbon cracking) process which consists in the integration of both reactions (endothermic n-butane cracking and exothermic methanol transformation) in a single fixed bed reactor, with the advantage that the integrated process can be performed under energy neutral conditions, which is interesting for simplifying the reactor design and improving the reactivity of n-butane.

Moreover, great attention has been paid in recent years to selective olefin production from methanol. The implementation of MTO process (methanol to olefins) units (on SAPO-34) is spreading, by obtaining methanol from natural gas (via synthesis gas) [32,33]. The results in the literature on the mechanism of the MTO process [34–37], and on the deactivation by coke of different catalysts (SAPO-34, SAPO-18 and HZSM-5 zeolites with different modifications) [38,39] allow predicting favourable synergies between the reactions of paraffin cracking and methanol transformation.

The CMHC process is interesting from the perspective of the petrochemical industry's sustainability. Methanol can be synthesised from various alternative sources to oil (natural gas, coal or biomass) via synthesis gas [40]. Furthermore, surplus paraffins in refinery streams are also valorised.

2. Experimental

2.1. Reaction equipment and product analysis

The runs have been carried out under atmospheric pressure in automated reaction equipment, Fig. 2. The operating variables are controlled by bespoke software (Processa).

The reactor is made of 316 stainless steel with an internal diameter of 9 mm and 10 cm of effective length. It is located inside a ceramic covered stainless steel cylindrical chamber, which is heated by an electric resistance, and can operate up to 100 atm and 700 °C with a catalyst mass of up to 5 g. The bed consists of a mixture of catalyst and inert solid (carborundum with an average particle diameter of 0.16 mm) to ensure bed isothermality and attain sufficient height under low space time conditions. The temperature is controlled by a digital TTM-125 Series controller and measured by a thermocouple (K type) located in the catalyst bed.

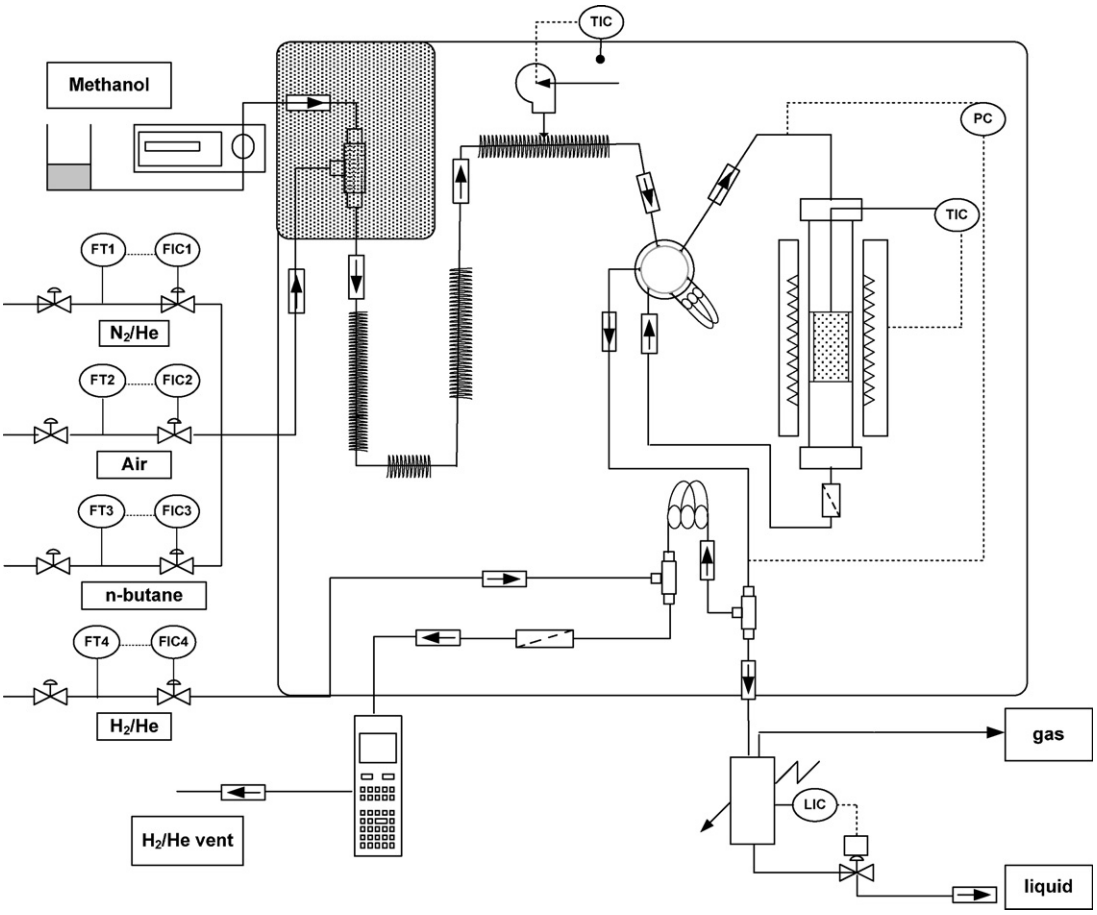

Fig. 2. Reaction equipment.

There are two other temperature controllers: one for the furnace chamber and the other for the transfer line between the reactor and the gas chromatograph (micro-GC Varian CP-4900).

At the end of each run, temperature is kept constant and catalyst sweeping is carried out with a helium flow of 30 $cm^3\,min^{-1}$ for 30 min, stabilizing and homogenizing the coke deposited on the catalyst for further analysis.

Reaction product samples (diluted in a He stream of 17 $cm^3\,min^{-1}$) are continuously analyzed in the gas chromatograph. The remaining stream of reaction products passes through a Peltier cell at 0 °C. The amount of liquid condensate is controlled by a level sensor, and the non-condensable gas flow is vented.

The gas chromatograph (with Star Toolbar software) is provided with 3 analytical modules and the following columns: Porapak Q (PPQ) (10 m), where the lighter products are separated (CO_2, methane, ethane, ethylene, propane, propylene, methanol, dimethyl ether, water, butanes and butenes); a molecular sieve (MS-5) (10 m) where H_2, CO, O_2 and N_2 are separated; and 5CB (CPSIL) (8 m), where C_5–C_{10} fraction is separated. The compounds were quantified and identified using calibration standards of known concentration. The balance of atoms (C, H, O) is closed in all runs above 99.5%.

2.2. Catalyst

The catalyst has been selected in a previous paper based on the combination of different criteria (activity at zero time on stream, olefin selectivity, deactivation by coke deposition and hydrothermal stability) [41]. The selected catalyst (HZ-30) has been prepared based on a HZSM-5 zeolite with $SiO_2/Al_2O_3 = 30$ that, supplied by Zeolyst International in ammonium form, has been calcined at 570 °C in order to obtain the acid form.

The zeolite has been agglomerated with a binder (bentonite Exaloid) (30 wt%) and alumina (Prolabo, calcined at 1000 °C to render it inert) as inert charge (45 wt%). The catalyst particles have been obtained by wet extrusion, using a high-pressure hydraulic piston (manufactured and supplied by Roquet, Spain), through 0.8 mm diameter holes. The extrudates are first dried at room temperature for 24 h, then they are sieved to a particle diameter between 0.3 and 0.15 mm. The particles are dried in an oven at 110 °C for 24 h and then calcined at 575 °C for 3 h. This temperature is reached following a ramp of 5 °C min^{-1}. The agglomeration of the active phases does not significantly reduce acidity, but improves the accessibility of the reactants (providing the catalysts with a matrix with meso- and macropores), which is essential for reducing deactivation by coke deposition and increasing hydrothermal stability in the regeneration step by coke combustion [42].

Other authors have identified the problem of irreversible deactivation of the catalyst as one of the greatest difficulties in the CMHC process [43–45]. This problem has been studied in a previous paper in which the used catalyst has been proven to recover its activity for up to 10 reaction–regeneration cycles without observing irreversible deactivation either in the reaction stage or in the regeneration stage, with the latter being performed in situ by coke combustion with air in the reactor at 550 °C [46].

Table 1 sets out the physical properties and the acidity values of the catalyst. The porous structure has been determined by N_2 adsorption–desorption (Micromeritics ASAP 2010) and Hg porosimetry (Micromeritics Autopore 9220). The micropore volume corresponds to the active phase, whereas the volume of meso-

Table 1
Physical properties and acidity of the catalyst.

Acid strength (kJ(mol$_{NH_3}$)$^{-1}$)	Total acidity (mmol$_{NH_3}$ g^{-1})	d_p (Å)	S_{BET} (m^2 g^{-1})	V_m (cm^3 g^{-1})	V_p (cm^3 g^{-1}) 17 < d_p(Å) < 3000
120	0.23	102	220	0.044	0.69
Pore volume distribution (%) <20/20 < d_p(Å) < 500/>500		Brönsted/Lewis ratio at 150 °C			
2.96/46.5/50.5		1.50			

and macropores correspond to the matrix of the catalyst (bentonite and alumina).

The total acidity and acid strength of the catalyst have been determined by monitoring the adsorption–desorption of NH_3, by combining the techniques of thermo-gravimetric analysis and differential scanning calorimetry using a Setaram TG–DSC calorimeter connected on-line to a Thermostar mass spectrometer from Balzers Instruments [47]. The Brönsted/Lewis (B/L) acid site ratio has been determined by analyzing the region of 1400–1700 cm^{-1} in the FTIR spectrum of adsorbed pyridine, which has been obtained using a Specac catalytic chamber connected on-line to a Nicolet 6700 FTIR spectrometer. Fig. 3 shows the FTIR spectra of pyridine adsorbed at 150 °C.

The Brönsted/Lewis site ratio value at 150 °C has been determined from the ratio between the intensity of pyridine adsorption bands at 1545 cm^{-1} and 1450 cm^{-1} and taking into account the molar extinction coefficients of both adsorption bands given by Emeis (ε_B = 1.67 cm μmol^{-1} and ε_L = 2.22 cm μmol^{-1}) [48].

3. Results

3.1. Reactant ratio for an energy neutral process

Fig. 4 shows the contour maps for the heat released (kJ(mol$_{CH_2}$)$^{-1}$) in the integrated process for different combinations of temperature and methanol/n-butane molar ratios in the feed. A computer program written in MATLAB based on a methodology established in the literature has been used [49,50]. As observed, the integrated process is exothermic for high methanol/n-butane molar ratios and moderate temperatures, whereas the opposite conditions correspond to an endothermic behaviour. At 550 °C and a methanol/n-butane molar ratio of 3/1 the process is energy neutral.

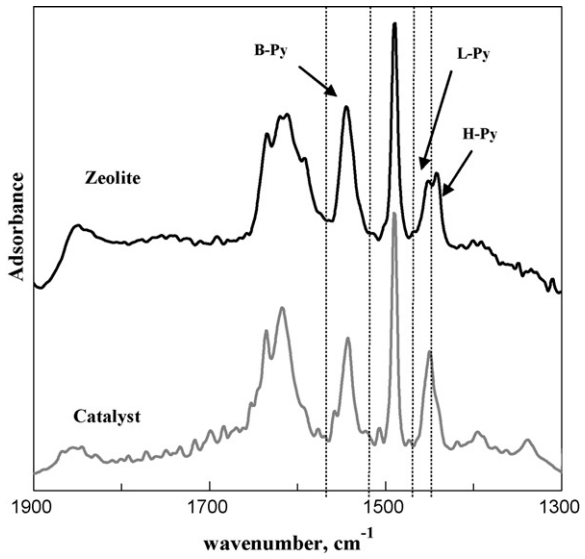

Fig. 3. FTIR spectra of pyridine adsorbed at 150 °C on the catalyst and on the HZSM-5 zeolite used for its preparation.

3.2. Improvements in the product distribution

The operating conditions in the integrated process are: pressure, atmospheric; methanol/n-butane ratios in the feed (in CH_2 equivalent units), up to 4; temperature, between 400 and 575 °C; space time, up to 9.5 (g of catalyst) h (mol CH_2)$^{-1}$; time on stream, 4 h. The individual reactions of n-butane cracking and methanol transformation have been studied for values of space time of up to 2.4 (g of catalyst) h (mol CH_2)$^{-1}$; the remaining conditions are the same as those used in the integrated process.

The following lumps of products have been studied: light olefins (ethylene, propylene and butanes), light paraffins (ethane, propane and isobutene), C_{5+} aliphatics (olefins and paraffins), aromatics (benzene, toluene and xylenes) and methane.

The integrated process features conditions under which n-butane behaves as both reactant and reaction product, the latter formed in the transformation of methanol. When conversions are defined in the integrated process for oxygenates and n-butane, in the latter case they are negative for certain operating conditions, which has no physical meaning. Therefore, an apparent conversion has been defined for the combined feed (n-butane/oxygenates):

$$X_{\text{apparent}} = \frac{F_0 - F_e}{F_0} \quad (1)$$

where F_0 and F_e correspond to oxygenates + n-butane flowrate calculated as CH_2 equivalent moles at the inlet and outlet of the reactor.

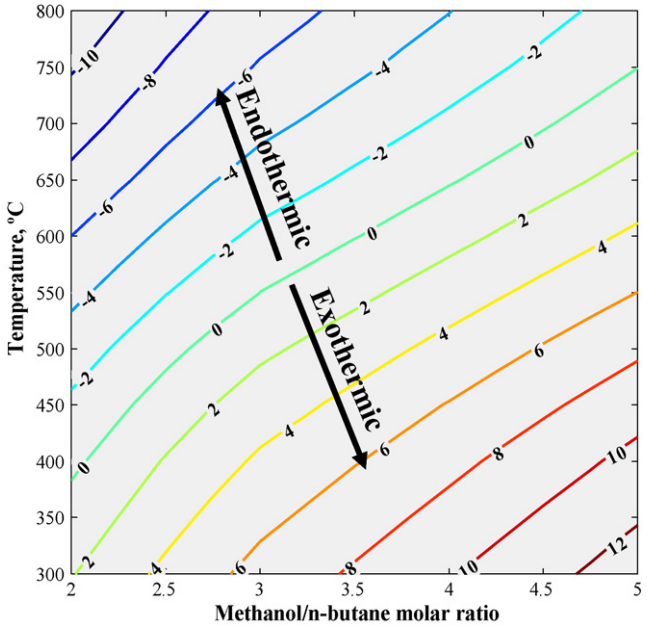

Fig. 4. Contour map of heat released (kJ (mol CH_2)$^{-1}$) in the integrated process for different combinations of temperature and methanol/n-butane molar ratio in the feed.

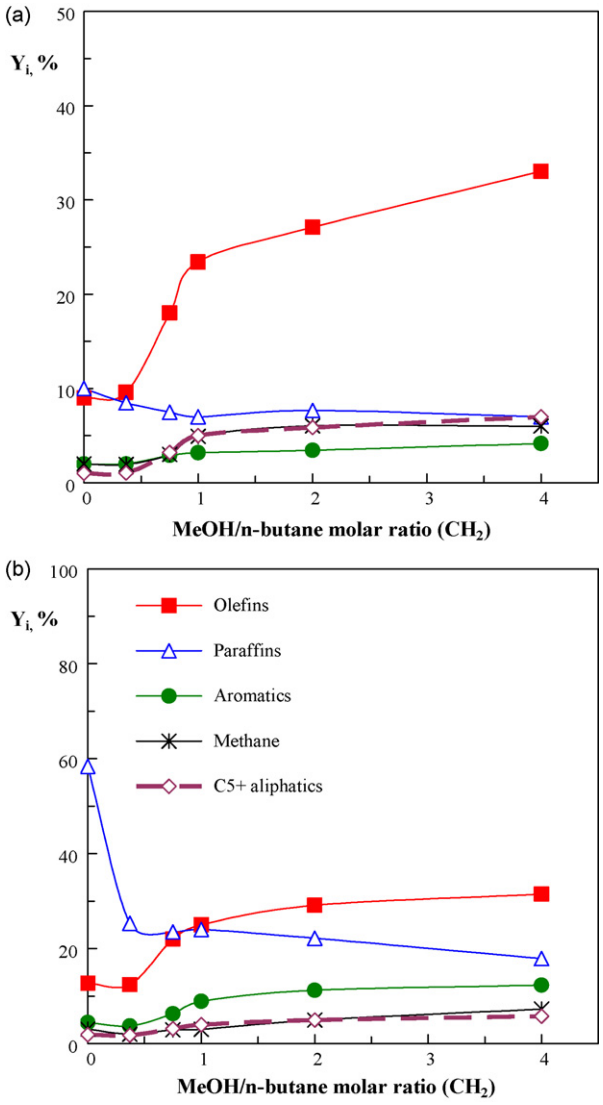

Fig. 5. Effect of methanol/n-butane molar ratio (CH_2 equiv. units) in the feed on the yield of reaction products at zero time on stream, 550 °C. (a) Space time, 0.24 (g of catalyst) h (mol of CH_2)$^{-1}$; (b) space time, 2.4 (g of catalyst) h (mol of CH_2)$^{-1}$.

The yield of each lump has been calculated as:

$$Y_i = \frac{F_i}{F_0} \quad (2)$$

where F_i is the molar flowrate of the i lump in the product stream expressed in CH_2 units.

Fig. 5 shows the effect of methanol/n-butane molar ratio in the feed (in CH_2 equivalent units) on the yield of reaction product lumps at zero time on stream by extrapolation of product yield evolution with time. The results correspond to 550 °C and each graph to a space time value. The yield of C_2–C_4 olefins increases significantly as the methanol/n-butane ratio is increased to a range of 0.75–1.0 (in CH_2 equiv. units), whereas the yield of C_2–C_4 paraffins decreases in the same range (Fig. 5a). This effect is more pronounced for higher values of space time, 2.4 (g of catalyst) h (mol CH_2)$^{-1}$ (Fig. 5b). Under these conditions, an increase in aromatic yield is also considerable as the methanol/n-butane ratio increases, although it is less pronounced than that of C_2–C_4 olefins.

These results are explained primarily by the energy compensation of the two reactions, the transformation of n-butane (endothermic) and the transformation of methanol (exothermic), so that increasing the methanol/n-butane ratio in the feed will presumably increase the real temperature in the acid centres, although local temperature on the active sites clearly cannot be measured. Furthermore, when increasing the methanol/n-butane ratio in the feed the water formed as a product of methanol dehydration will help to decrease the C_2–C_4 paraffin yield. This hypothesis is consistent with that of Corma et al. [51], who attribute the higher yield of olefins in n-hexadecane cracking by co-feeding water to the enhancement of n-hexadecane diffusion in the zeolite crystal channels and to the attenuation of bimolecular cracking and hydrogen transfer reactions, which lead to the formation of paraffins.

Moreover, the yield of C_2–C_4 paraffins in the integrated process is much lower than that determined in a previous work (60 wt%), where the cracking of n-butane was studied under similar reaction conditions, which confirms the effect of water in the reaction medium [41].

The methanol/n-butane molar ratio corresponding to the inflexion point in the curve of olefin yield shown in Fig. 5 is 0.75–1.0 (based on CH_2 units) which corresponds to a methanol/n-butane molar ratio of 3/1, for which the two reactions are energy balanced according to thermodynamics (Fig. 4).

The results in Fig. 5 indicate an important advantage of the integrated process over methanol transformation concerning the reduction in by-products and greenhouse gases. In the transformation of methanol above 500 °C, the thermal decomposition of methanol is significant, with the formation of methane, CO and CO_2. The methane yield in the integrated process is significantly lower than that obtained with a similar catalyst in methanol transformation, particularly when the catalyst is partially deactivated [38–52]. The yield of CO + CO_2 is also lower than in the transformation of methanol and barely reaches 0.5% (C transformed) at the maximum temperature, 575 °C, and for the minimum value of space time studied.

This attenuation of the reactions involving methanol thermal decomposition is because they occur simultaneously to the endothermic cracking of n-butane, and this avoids the formation of hot spots in the vicinity of the catalyst active sites.

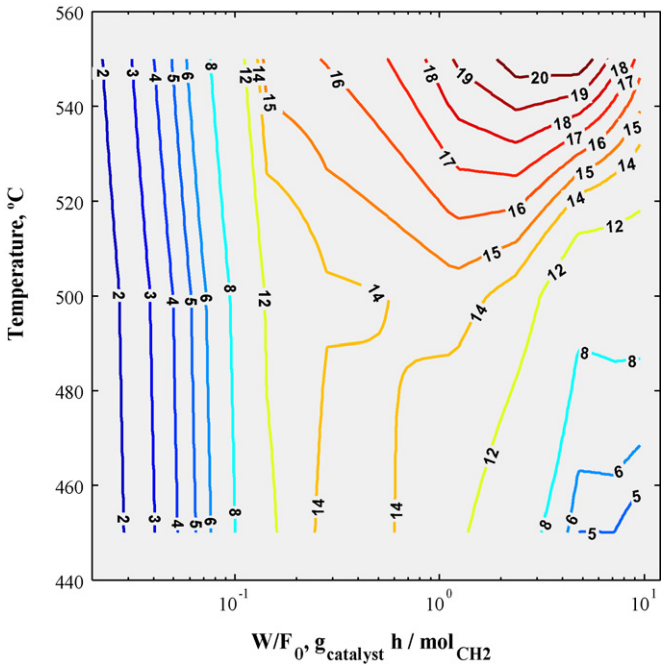

Fig. 6. Contour map for the yields of C_2–C_4 olefins (express in % of CH_2 equiv. units) in the joint transformation of methanol and n-butane for different possible combinations of temperature and space time.

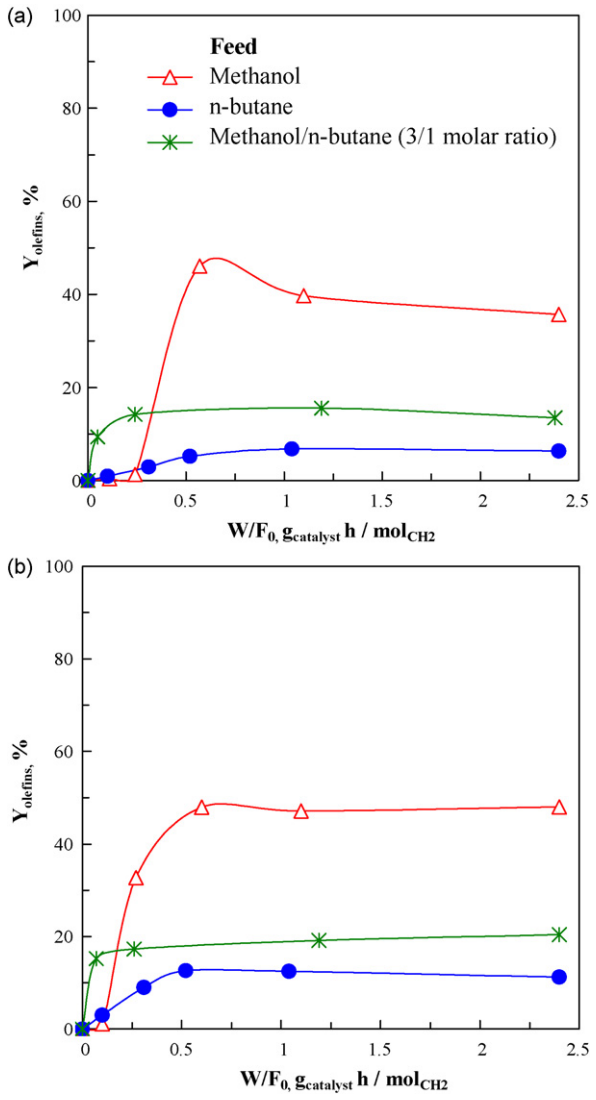

Fig. 7. Comparison of the effect of space time on C_2–C_4 olefin yield in the methanol transformation process, n-butane cracking and in the integrated process (methanol/n-butane molar ratio = 3/1), at 500 °C (a) and 550 °C (b).

3.3. Conditions for olefin production

Fig. 6 shows the contour maps for C_2–C_4 olefin yield (expressed in CH_2 unit percentage) for different combinations of temperature and space time in the integrated process. The data plotted correspond to the values extrapolated at zero time on stream of yield evolution with time on stream for different reaction conditions. There is a region of optimum yield for temperatures above 540 °C and space times between 2 and 5 (g of catalyst) h (mol CH_2)$^{-1}$, in which C_2–C_4 olefin yields are above 20%.

3.4. Synergy in olefin production

The effect of space time on the yield of C_2–C_4 olefins in n-butane cracking, methanol transformation and the integrated process is compared in Fig. 7. The results correspond to 500 °C (Fig. 7a) and to 550 °C (Fig. 7b). It is observed that for both temperatures studied methanol transformation requires an autocatalytic or acceleration step in the generation of olefins. Consequently, a space time higher than 0.25 (g of catalyst) h (mol CH_2)$^{-1}$ is required at 500 °C for olefin formation. At 550 °C, the space time required for olefin formation is lower, around 0.10 (g of catalyst) h (mol CH_2)$^{-1}$.

Olefin formation in the integrated process is almost direct. This is explained by the presence in the reaction medium of C_2–C_4 olefins produced in the cracking of n-butane from very low values of space time. These olefins activate the "hydrocarbon pool" mechanism established for the transformation of methanol into hydrocarbons [34,35]. In this mechanism C_2–C_4 olefins are released from intermediate compounds (polymethylbenzenes) or from the corresponding cations, which in turn also evolve into coke precursors that deactivate the catalyst [53]. The presence of these intermediates has been confirmed by different spectroscopic methods [54–57], and their formation prior to that of olefins explains the existence of an initiation period whose duration decreases as temperature is increased and water content in the reaction medium is decreased [36]. Bjorgen et al. [37] have proposed a mechanism of "double cycle" for the formation of olefins on HZSM-5 zeolite, in which polymethylbenzenes are less active than on SAPO-34 and on β-zeolite. According to this mechanism, ethylene is released in cycle I from polymethylbenzene formed by methylation of aromatics. C_{3+} olefins are formed in cycle II by methylation-cracking of olefins, at the same time generating aromatics by cyclization of naphthenes and subsequent hydrogen transfer, which activates cycle I.

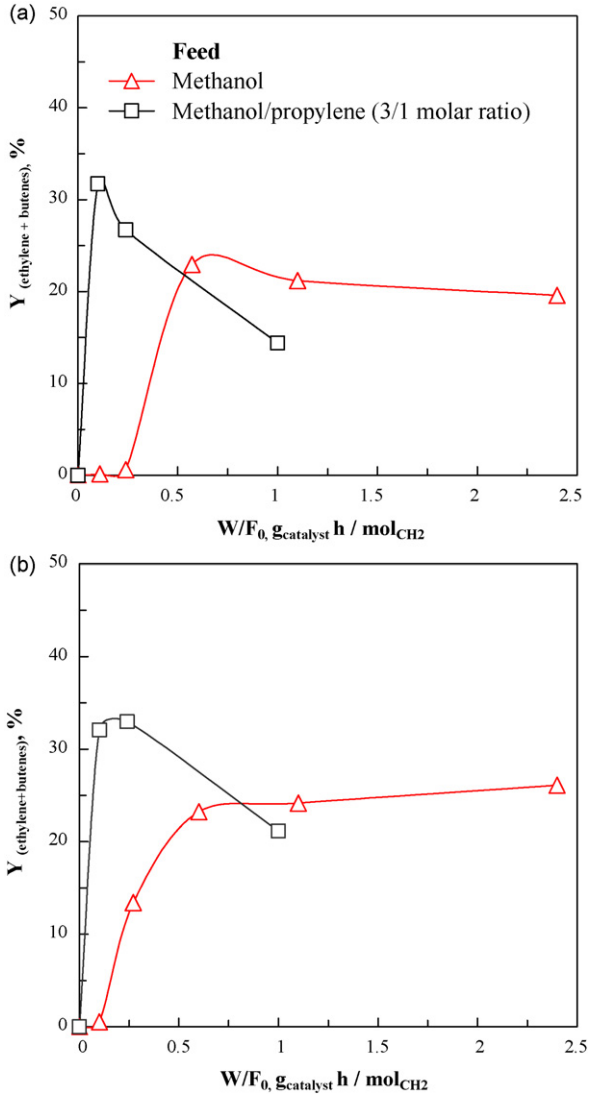

Fig. 8. Effect of propylene co-feeding with methanol on ethylene + butenes yield for different values of space time, at 500 °C (a) and 550 °C (b).

This result of the integrated process is relevant in order to transform methanol with a small value of space time. Furthermore, it has already been confirmed that co-feeding olefins with methanol activates the formation of olefins [34,35,58]. In order to verify this finding for our catalyst and operating conditions, a mixture of methanol and propylene (3/1 molar ratio) has been fed into the reactor.

Fig. 8 compares the yields of ethylene + butenes obtained by feeding methanol and the mixture of methanol/propylene for different values of space time. Fig. 8a corresponds to 500 °C and Fig. 8b to 550 °C. The results show that when co-feeding propylene the formation of ethylene and butenes requires a very small value of space time. However, it is also observed that by increasing space time the mixture gives way to lower yields than those obtained when pure methanol is fed.

From an industrial point of view the integrated process is interesting for maximizing the selectivity of C_2–C_4 olefins, which has been calculated as the ratio of their molar flowrate in the product stream to the sum of olefin flowrate and non-recyclable product flowrate, F_{NR}, in the output stream.

$$S_{olefins} = \frac{F_{olefins}}{F_{olefins} + F_{NR}} 100 \quad (3)$$

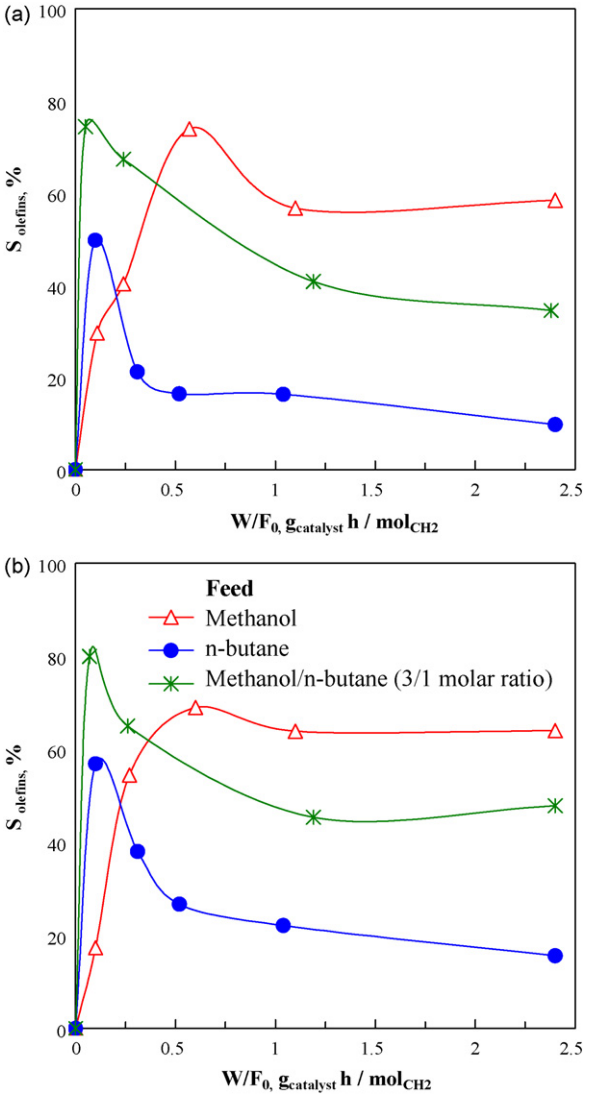

Fig. 9. Comparison of the evolution with space time of C_2–C_4 olefin selectivity in methanol transformation process, n-butane cracking and in the integrated process (methanol/n-butane molar ratio = 3/1), at 500 °C (a) and 550 °C (b).

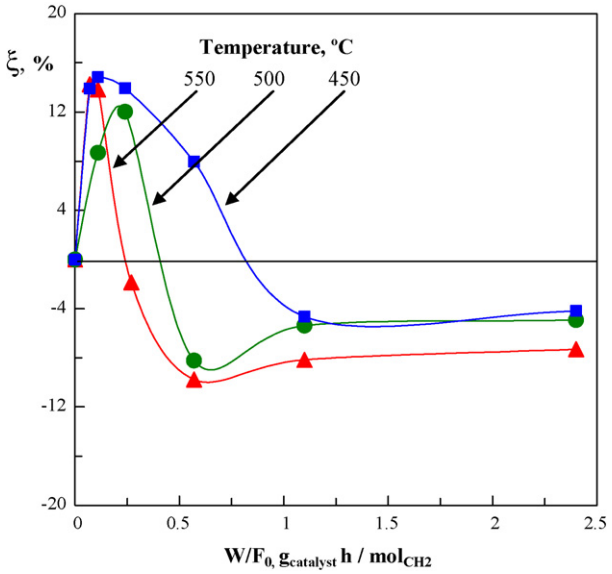

Fig. 10. Improvement coefficient in the integrated process for different values of space time and three values of temperature.

The definition of selectivity based on recyclable products is useful in this process and in others, such as the MTO process, for which industrial operation is conducted by recycling a fraction of the product stream.

The products considered in Eq. (3) to be recycled back into the reactor for olefin production are: (i) non-aromatic C_4–C_{10} fraction, whose reactivity for cracking is similar to or higher than that of n-butane and; (ii) dimethyl ether, whose reactivity in the MTO process is higher than that of methanol [59].

The results of C_2–C_4 olefin selectivity are shown in Fig. 9 and correspond to 500 °C (Fig. 9a) and 550 °C (Fig. 9b). As observed, C_2–C_4 olefin selectivity in the integrated process is very high. A maximum selectivity of 80% is obtained for a low value of space time, around 0.1–0.2 (g of catalyst) h $(mol\,CH_2)^{-1}$, at the two temperatures (500 and 550 °C), which is also the case in n-butane cracking, although the selectivity in this reaction decreases sharply as space time is increased, but in the integrated process the decrease is more attenuated.

In order to quantify the improvement in the joint feeding of n-butane and methanol, a coefficient, ξ, has been defined as the difference between the olefin yields in the integrated process, $Y^{CMHC}_{olefins}$, and those obtained assuming these two reactions are carried out separately. These virtual yields in methanol transformation, $Y^{MTO}_{olefins}$, and n-butane cracking, $Y^{BC}_{olefins}$, have been calculated assuming that the individual processes occur independently for the same value of space time. The calculation for the integrated process takes into account that methanol/n-butane ratio = 3/4 in the feed based on CH_2 equivalent units (methanol/n-butane = 3/1 molar ratio). Based on these considerations, the improvement coefficient is calculated as:

$$\xi = Y^{CMHC}_{olefins} - (0.43Y^{MTO}_{olefins} + 0.57Y^{BC}_{olefins}) \quad (4)$$

Fig. 10 shows the improvement coefficient of the integrated process, ξ, at zero time on stream, for different values of space time and for three values of temperature. As observed in the integrated process for small values of space time, olefin yield is higher than when the reactions are carried out individually, which is due to the aforementioned activation of the methanol transformation mechanism by the presence of olefins produced by n-butane cracking in the reaction medium. This improvement is lower as temperature is increased, which is because the

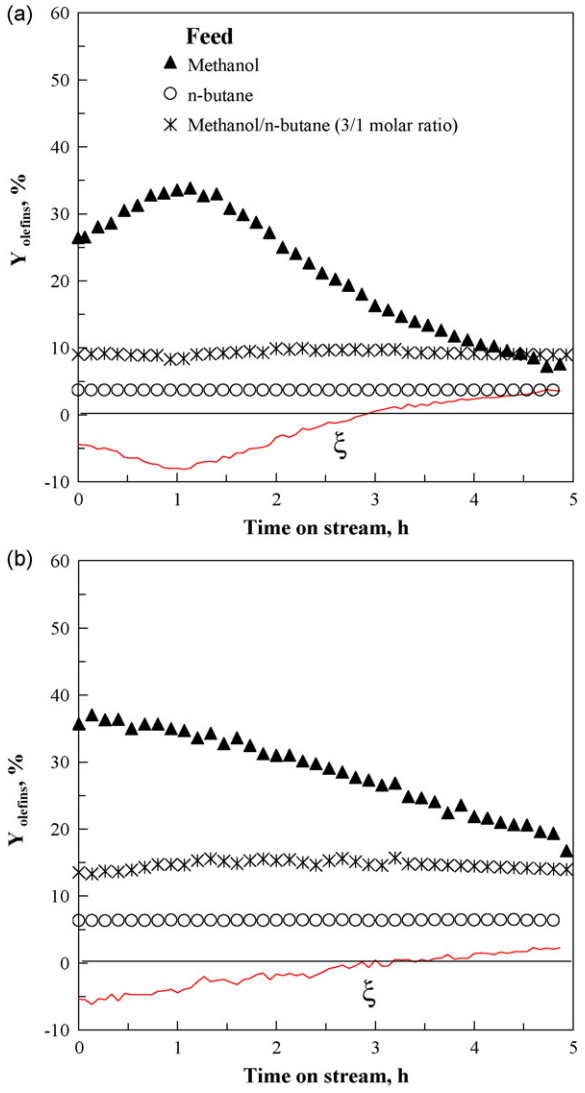

Fig. 11. Comparison of the evolution with time on stream of olefin yield in the methanol transformation process, n-butane cracking and in the integrated process (methanol/n-butane molar ratio = 3/1) and evolution of the improvement coefficient in the integrated process for 2.4 (g of catalyst) h (mol CH_2)$^{-1}$, at 450 °C (a) and 500 °C (b).

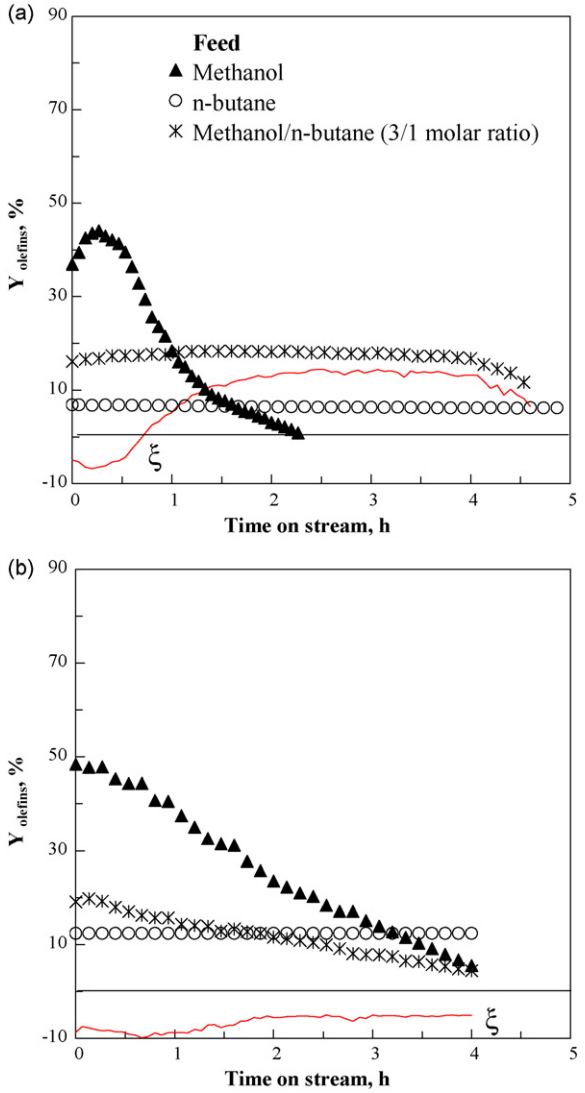

Fig. 12. Comparison of the evolution with time on stream of olefin yield in the methanol transformation process, n-butane cracking and in the integrated process (methanol/n-butane molar ratio = 3/1) and evolution of the improvement coefficient in the integrated process for 1.1 (g of catalyst) h (mol CH_2)$^{-1}$, at 500 °C (a) and 550 °C (b).

mechanism of formation and activation of the intermediates in methanol transformation into hydrocarbons is faster when temperature is increased [37,47]. Moreover, for high values of space time, lower olefin yields are obtained when feeding the mixture than those that would be obtained by performing the individual reactions, given that under these conditions the formation of hydrocarbons is enhanced in the transformation of methanol and the main effect of co-feeding n-butane is the undesired dilution of methanol.

3.5. Attenuation of the deactivation

Figs. 11 and 12 compare the evolution with time on stream, and therefore with the progress of catalyst deactivation, of C_2–C_4 olefin yield in n-butane cracking, methanol transformation and in the integrated process. The evolution with time on stream of the improvement coefficient, ξ, is also shown, which is calculated by Eq. (4) from the results of evolution with time on stream of olefin yields in the three processes. The results in Fig. 11 correspond to a space time of 2.4 (g of catalyst) h (mol CH_2)$^{-1}$ (Fig. 11a at 450 °C and Fig. 11b at 500 °C) and those in Fig. 12 to 1.1 (g of catalyst) h (mol CH_2)$^{-1}$ (Fig. 12a at 500 °C and Fig. 12b at 550 °C).

For the values of space time in Figs. 11 and 12, the improvement coefficient is negative for zero time on stream (as occurred in Fig. 10 for suitable high values of space time). Nevertheless, this coefficient increases for values of time on stream higher than those corresponding to the peak of olefin yield in the transformation of methanol. The improvement coefficient is positive above 3 h and increases as time on stream is increased for a space time of 2.4 (g of catalyst) h (mol CH_2)$^{-1}$ (Fig. 11), and above 1 h for a space time of 1.1 (g of catalyst) h (mol CH_2)$^{-1}$ and 500 °C (Fig. 12a). However, as observed in Fig. 12b corresponding to 550 °C, the improvement coefficient is not positive for 4 h of time on stream, which is because the deactivation in the reaction of methanol transformation at this temperature is very high and this negatively affects the n-butane cracking reaction that requires strong acid centres.

The aforementioned results show that the integrated process has a positive effect by mitigating the deactivation rate of the catalyst, which is fast in the reaction of methanol transformation on HZSM-5 zeolite for small values of space time. The deactivation

rate of HZSM-5 zeolite by coke deposition in the transformation of methanol has been extensively studied, and its lower deactivation compared to other catalysts is noteworthy [47,52,60]. This good performance of HZSM-5 zeolite is attributed to a suitable balance of its properties: (i) moderate shape selectivity; (ii) three-dimensional structure of micropores, without cages in the channel intersections, and; (iii) moderate acid strength of the centres [61–63]. Nevertheless, it should be noted that the temperature at which the integrated process has been studied in this paper is higher than that normally used in the transformation of methanol into hydrocarbons (<450 °C) and, therefore, deactivation conditions are more severe. The attenuation of deactivation is presumably due to the favourable effect of a higher amount of C_2–C_4 olefins (n-butane cracking products) on the mechanism of olefin formation from the aforementioned polymethylbenzenes, given that the coke is formed from the evolution of polymethylbenzenes towards inactive polyaromatic structures [37].

4. Conclusions

The integration of n-butane cracking (endothermic reaction) and methanol transformation (exothermic reaction) in the same reactor with a HZSM-5 zeolite allows performing the integrated process under energy-neutral conditions (with a methanol/n-butane molar ratio of 3 in the feed) with a high yield of C_2–C_4 olefins, and particularly propylene.

There are interesting synergies between the two individual reactions, which significantly reduce the limitations of each individual one. Co-feeding methanol with n-butane increases the temperature of the acid centres, since the exothermic conversion of methanol into hydrocarbons compensates the endothermic cracking. Furthermore, the presence of water in the reaction medium (product of methanol dehydration) contributes to attenuating the bimolecular cracking reactions and hydrogen transfer, favouring the selectivity of C_2–C_4 olefins. On the other hand, energy compensation is effective for mitigating the stages of thermal decomposition of methanol leading to unwanted products such as methane, CO and CO_2.

Furthermore, the presence in the reaction medium of C_2–C_4 olefins produced in n-butane cracking from low values of space time activates the formation of the intermediates for methanol transformation into hydrocarbons. Similarly, the presence of olefins contributes to reducing catalyst deactivation by coke, which is very rapid in the transformation of methanol. Consequently, the integrated process can be performed for higher values of time on stream than methanol transformation.

The energy compensation and synergies mentioned are especially appropriate for selectively obtaining C_2–C_4 olefins. The increase in their yield over those of the individual processes has been quantified with a coefficient, which is positive for low values of space time (suitable for maximizing the formation of C_2–C_4 olefins and particularly propylene). The selectivity of C_2–C_4 olefins at zero time on stream is very high, with a maximum value of 80% at 500–550 °C and very low space time, about 0.1–0.2 (g of catalyst) h (mol CH_2)$^{-1}$.

The integrated process means a route for the joint upgrading of two feeds, paraffins and methanol. The former are provided by secondary interest refinery streams and the latter is a key intermediate product for the valorisation via syngas of oil alternative sources, amongst which lignocellulosic biomass is an interesting one for preserving the environment. Although the study in this paper was conducted with n-butane, the yield of C_2–C_4 olefins is expected to be higher with heavier paraffins, since their reactivity in cracking will be higher than that of n-butane.

Nomenclature

ξ	improvement coefficient in olefin yield, Eq. (4)
d_p	mean pore diameter (Å)
F_0, F_e	molar flowrate of n-butane + oxygenates at the inlet and outlet of the reactor, respectively, CH_2 equivalent (mol h^{-1})
F_i, $F_{olefins}$	molar flowrate of i component and olefins in the output stream, CH_2 equivalent (mol h^{-1})
F_{NR}	molar flowrate of non-recyclable products in the output stream, CH_2 equivalent (mol h^{-1})
S_{BET}	BET surface area (m^2 g^{-1})
$S_{olefins}$	selectivity of olefins, Eq. (3)
V_m, V_p	micropore and pore volume (cm^3 g^{-1})
W	catalyst mass (g)
$X_{apparent}$	apparent conversion of n-butane + oxygenates, Eq. (1)
Y_i, $Y_{olefins}$	yield of i component, Eq. (2), and olefins
$Y^{BC}_{olefins}$	olefin yield in n-butane cracking in CH_2 equivalent units (mol of olefins) (mol in the feed)$^{-1}$
$Y^{CMHC}_{olefins}$	olefin yield in the integrated process in CH_2 equivalent units (mol of olefins) (mol in the feed)$^{-1}$
$Y^{MTO}_{olefins}$	olefin yield in methanol transformation in CH_2 equivalent units (mol of olefins) (mol in the feed)$^{-1}$

Acknowledgements

This work was carried out with the financial support of the Department of Education, Universities and Research of the Basque Government (Project GIC07/24-IT-220-07) and of the Ministry of Science and Innovation of the Spanish Government (Project CTQ2007-66571/PPQ).

References

[1] G.A. Olah, Beyond oil and gas: the methanol economy, Angew. Chem. Int. Ed. 44 (2005) 2636–2639.
[2] G.A. Olah, A. Goeppert, G.K.S. Prakash, Beyond Oil and Gas: The Methanol Economy, Willey-VCH, Weinheim, Germany, 2006.
[3] A. Corma, G.W. Huber, L. Sauvanaud, P. O'Connor, Processing biomass-derived oxygenates in the oil refinery: catalytic cracking (FCC) reaction pathways and role of catalyst, J. Catal. 247 (2007) 307–327.
[4] G.W. Huber, P. O'Connor, A. Corma, Processing biomass in conventional oil refineries: production of high quality diesel by hydrotreating vegetable oils in heavy vacuum oil mixtures, Appl. Catal. A: Gen. 329 (2007) 120–129.
[5] T. Ren, B. Daniels, M.K. Patel, K. Blok, Petrochemicals from oil, natural gas, coal and biomass: production costs in 2030–2050, Resour. Conserv. Recycl. 53 (2009) 653–663.
[6] T. Ren, M. Patel, K. Blok, Olefins from conventional and heavy feedstocks: energy use in stream cracking and alternative processes, Energy 31 (2006) 425–451.
[7] A. Raichle, Y. Traa, F. Fuder, M. Rupp, J. Weitkamp, Improving the field of ethene in the steamcracker by recycling of pyrolysis gasoline using Pd-, Pt-, Ir- or Ga-doped zeolites ZSM-5, Oil Gas J. Eur. Mag. 29 (2003) 33–36.
[8] T. Ren, M. Patel, K. Blok, Steam cracking and methane to olefins: energy use, CO_2 emissions and production costs, Energy 33 (2008) 817–833.
[9] J.M. Arandes, I. Abajo, I. Fernández, M.J. Azkoiti, J. Bilbao, Effect of HZSM-5 zeolite addition to a fluid catalytic cracking catalyst. Study in a laboratory reactor operating under industrial conditions, Ind. Eng. Chem. Res. 39 (2000) 1917–1924.
[10] J.S. Buchanan, The chemistry of olefins production by ZSM-5 addition to catalytic cracking units, Catal. Today 55 (2000) 207–212.
[11] A. Corma, F.V. Melo, L. Sauvanaud, F. Ortega, Light cracked naphtha processing: controlling chemistry for maximum propylene production, Catal. Today 107–108 (2005) 699–706.
[12] G. Wang, C. Xu, J. Gao, Study of cracking FCC naphtha in a secondary riser of the FCC unit for maximum propylene production, Fuel Process. Technol. 89 (2008) 864–873.
[13] X. Dupain, R.A. Krul, C.J. Schaverien, M. Makkee, J.A. Moulijn, Production of clean transportation fuels and lower olefins from Fischer–Tropsch synthesis waxes under fluid catalytic cracking conditions—the potential of highly paraffinic feedstocks for FCC, Appl. Catal. B: Environ. 63 (2006) 277–295.
[14] M.L. Fernández, G. de la Puente, A. Lacalle, J. Bilbao, U. Sedran, J.M. Arandes, Recycling hydrocarbon cuts into FCC units, Energy Fuels 16 (2002) 615–621.

[15] I. Torre, J.M. Arandes, M.J. Azkoiti, M. Olazar, J. Bilbao, Cracking of coker naphtha with gas–oil. Effect of HZSM-5 zeolite addition to the catalyst, Energy Fuels 21 (2007) 11–18.
[16] J.M. Arandes, I. Torre, M.J. Azkoiti, J. Ereña, J. Bilbao, Effect of atmospheric residue incorporation in the fluidized catalytic cracking (FCC) feed on product stream yields and composition, Energy Fuels 22 (2008) 2149–2156.
[17] Y. Fujiyama, H.H. Redhwi, A. Aitani, R. Saeed, C. Dean, Demonstration plant for new FCC technology yields increased propylene, Oil Gas J. 103 (2005) 54–58.
[18] J.M. Arandes, J. Ereña, J. Bilbao, D. López-Valerio, G. de la Puente, Valorization of polyolefins disolved in light cycle oil over HY zeolites under fluid catalytic cracking unit conditions, Ind. Eng. Chem. Res. 42 (2003) 3952–3961.
[19] J.M. Arandes, J. Ereña, M. Olazar, J. Bilbao, G. de la Puente, Valorization of the blends polystyrene/light cycle oil and polystyrene-butadiene/light cycle oil over different HY zeolites under FCC unit conditions, Energy Fuels 18 (2004) 218–227.
[20] J.M. Arandes, I. Torre, P. Castaño, M. Olazar, J. Bilbao, Catalytic cracking of waxes produced by the fast pyrolysis of polyolefins, Energy Fuels 21 (2007) 561–569.
[21] D. Sanfilippo, I. Miracca, Dehydrogenation of paraffins: synergies between catalyst design and reactor engineering, Catal. Today 111 (2006) 133–139.
[22] S.B. Wang, Z.H. Zhu, Catalytic conversion of alkanes to olefins by carbon dioxide oxidative dehydrogenation—a review, Energy Fuels 18 (2004) 1126–1139.
[23] A. Klisinska, K. Samson, I. Gressel, B. Grzybowska, Effect of additives on properties of V_2O_5/SiO_2 and V_2O_5/MgO catalysts I. Oxidative dehydrogenation of propane and ethane, Appl. Catal. A: Gen. 309 (2006) 10–16.
[24] A. Klisinska, S. Loridant, B. Grzybowska, J. Stoch, I. Gressel, Effect of additives on properties of V_2O_5/SiO_2 and V_2O_5/MgO catalysts II. Structure and physicochemical properties of the catalysts and their correlations with oxidative dehydrogenation of propane and ethane, Appl. Catal. A: Gen. 309 (2006) 17–27.
[25] J.P. Lange, R.J. Schoonebeek, P.D.L. Mercera, F.W. van Breukelen, Oxycracking of hydrocarbons: chemistry, technology and economic potential, Appl. Catal A: Gen. 283 (2005) 243–253.
[26] C.M. Naccache, P. Mériaudeau, G. Sapaly, L. Van Tiep, Y. Ben Taârit, Assessment of the low-temperature nonoxidative activation of methane over H-galloaluminosilicate (MFI) zeolite: a C-13 labelling investigation, J. Catal. 205 (2002) 217–220.
[27] J.H. Lunsford, Catalytic conversion of methane to more useful chemicals and fuels: a challenge for the 21st century, Catal. Today 63 (2000) 165–174.
[28] S. Bhatia, Ch.Y. Thien, A.R. Mohamed, Oxidative coupling of methane (OCM) in a catalytic membrane reactor and comparison of its performance with other catalytic reactors, Chem. Eng. J. 148 (2009) 525–532.
[29] J.S. Ahari, R. Ahmadi, H. Mikami, K. Inazu, S. Zarrinpashne, S. Suzuki, K. Aika, Application of a simple kinetic model for the oxidative coupling of methane to the design of effective catalysts, Catal. Today 145 (2009) 45–54.
[30] M.T. Ravanchi, T. Kaghazchi, A. Kargari, Application of membrane separation processes in petrochemical industry: a review, Desalination 235 (2009) 199–244.
[31] A. Martin, S. Nowak, B. Lücke, H. Günschel, Coupled conversion of methanol and C-4 hydrocarbons to lower olefins, Appl. Catal. 50 (1989) 149–155.
[32] J.Q. Chen, A. Bozzano, B. Glover, T. Fuglerud, S. Kvisle, Recent advancements in ethylene and propylene production using the UOP/Hydro MTO process, Catal. Today 106 (2005) 103–107.
[33] T.R. Keshav, S. Basu, Gas-to-liquid technologies: India's perspective, Fuel Process. Technol. 88 (2007) 493–500.
[34] I.M. Dahl, S. Kolboe, On the reaction-mechanism for propene formation in the MTO reaction over SAPO-34, Catal. Lett. 20 (1993) 329–336.
[35] I.M. Dahl, S. Kolboe, On the reaction-mechanism for hydrocarbon formation from methanol over SAPO-34. 1. Isotopic labelling studies of the co-reaction of ethane and methanol, J. Catal. 149 (1994) 458–464.
[36] A.T. Aguayo, A.G. Gayubo, R. Vivanco, A. Alonso, J. Bilbao, Kinetic behavior of the SAPO-18 catalyst in the transformation of methanol into olefins, Ind. Eng. Chem. Res. 44 (2005) 7279–7286.
[37] M. Bjorgen, S. Svelle, F. Joensen, J. Nerlov, S. Kolboe, F. Bonino, L. Palumbo, S. Bordiga, U. Olsbye, Conversion of methanol to hydrocarbons over zeolite H-ZSM-5: on the origin of the olefinic species, J. Catal. 249 (2007) 195–207.
[38] A.G. Gayubo, A.T. Aguayo, M. Olazar, R. Vivanco, J. Bilbao, Kinetics of the irreversible deactivation of the HZSM-5 catalyst in the MTO process, Chem. Eng. Sci. 258 (2003) 5239–5249.
[39] A.G. Gayubo, A.T. Aguayo, A. Alonso, J. Bilbao, Kinetic modeling of the methanol-to-olefins process on a silicoaluminophosphate (SAPO-18) catalyst by considering deactivation and the formation of individual olefins, Ind. Eng. Chem. Res. 46 (2007) 1981–1989.
[40] P.G. Cifre, O. Badr, Renewable hydrogen utilisation for the production of methanol, Energy Conserv. Manage. 48 (2007) 519–527.
[41] D. Mier, Obtención de olefinas por transformación catalítica de parafinas y methanol en un proceso integrado, Ph.D. Thesis, University of the Basque Country, Bilbao, Spain, 2009.
[42] P.L. Benito, A.T. Aguayo, A.G. Gayubo, J. Bilbao, Hydrocarbons by reaction-regeneration cycles, Ind. Eng. Chem. Res. 35 (1996) 2177–2182.
[43] A. Martin, S. Nowak, B. Lücke, W. Wieker, B. Fahlke, Coupled conversion of methanol and C-4 hydrocarbons (CMHC) on iron-containing ZSM-5 type zeolites, Appl. Catal. 57 (1990) 203–214.
[44] A. Martin, U. Wolf, S. Nowak, B. Lücke, Pyridine-IR investigations of hydrothermally treated dealuminated HZSM-5 zeolites, Zeolites 11 (1991) 85–92.
[45] B. Lücke, A. Martin, H. Günschel, S. Nowak, CMHC: coupled methanol hydrocarbon cracking—formation of lower olefins from methanol and hydrocarbons over modified zeolites, Microporous Mesoporous Mater. 29 (1999) 145–157.
[46] D. Mier, A.T. Aguayo, A.G. Gayubo, M. Olazar, J. Bilbao, Catalyst discrimination for olefin production by coupled methanol/n-butane cracking, Appl. Catal. A: Gen. Submitted for publication.
[47] A.T. Aguayo, A.G. Gayubo, R. Vivanco, M. Olazar, J. Bilbao, Role of acidity and microporous structure in alternative catalysts for the transformation of methanol into olefins, Appl. Catal. A. Gen. 283 (2005) 197–207.
[48] A.G. Gayubo, A.T. Aguayo, A. Atutxa, R. Prieto, J. Bilbao, Role of reaction-medium water on the acidity deterioration of a HZSM-5 zeolite, Ind. Eng. Chem. Res. 43 (2004) 5042–5048.
[49] J.M. Smith, H.C. Van Ness, M.M. Abbott, Introduction to Chemical Engineering Thermodynamics, 7th ed., McGraw-Hill, New York, 2005, p. 483.
[50] K. Denbigh, The Principles of Chemical Equilibrium: With Applications in Chemistry and Chemical Engineering, 4th ed., Cambridge University Press, Cambridge, United Kingdom, 1997, Chapter 4.
[51] A. Corma, O. Marie, F.J. Ortega, Interaction of water with the surface of a zeolite catalyst during catalytic cracking: a spectroscopy and kinetic study, J. Catal. 22 (2004) 338–347.
[52] P.L. Benito, A.G. Gayubo, A.T. Aguayo, M. Olazar, J. Bilbao, Deposition and characteristics of coke over a H-ZSM5 zeolite-based catalyst in the MTG process, Ind. Eng. Chem. Res. 35 (1996) 3991–3998.
[53] M. Guisnet, Coke molecules trapped in the micropores of zeolites as active species in hydrocarbon transformations, J. Mol. Catal. A: Chem. 182 (2002) 367–382.
[54] W. Song, J.F. Haw, J.B. Nicholas, C.S. Heneghan, Methylbenzenes are the organic reaction centers for methanol-to-olefin catalysis on HSAPO-34, J. Am. Chem. Soc. 122 (2000) 10726–10727.
[55] B. Arstad, S. Kolboe, Methanol-to-hydrocarbons reaction over SAPO-34. Molecules confined in the catalyst cavities at short time on stream, Catal. Lett. 71 (2001) 209–212.
[56] B. Arstad, S. Kolboe, The reactivity of molecules trapped within the SAPO-34 cavities in the methanol-to-hydrocarbons reaction, J. Am. Chem. Soc. 123 (2001) 8137–8138.
[57] Y. Jiang, J. Huang, R.V.R. Marthala, Y.S. Ooi, J. Weitkamp, M. Hunger, In situ MAS NMR-UV/Vis investigation of H-SAPO-34 catalysts partially coked in the methanol-to-olefin conversion under continuous-flow conditions and of their regeneration, Microporous Mesoporous Mater. 105 (2007) 132–139.
[58] J. Li, Y. Qi, L. Xu, G. Liu, S. Meng, B. Li, M. Li, Z. Liu, Co-reaction of ethene and methanol over modified H-ZSM-5, Catal. Commun. 9 (2008) 2515–2519.
[59] A.G. Gayubo, A.T. Aguayo, A.L. Morán, M. Olazar, J. Bilbao, Role of water in the kinetic modeling of catalyst deactivation in the MTG process, AIChE J. 48 (2002) 1561–1571.
[60] A.T. Aguayo, P.L. Benito, A.G. Gayubo, M. Olazar, J. Bilbao, Acidity deterioration and coke deposition in a HZSM-5 zeolite in the MTG process, Stud. Surf. Sci. Catal. 88 (1994) 567–572.
[61] M. Guisnet, P. Magnoux, Organic chemistry of coke formation, Appl. Catal. A: Gen. 212 (2001) 83–96.
[62] M. Guisnet, L. Costa, F.R. Ribeiro, Prevention of zeolite deactivation by coking, J. Mol. Catal. A: Chem. 305 (2009) 69–83.
[63] D. Mores, E. Stavitski, M.H.F. Kox, J. Kornatowski, U. Olsbye, B.M. Weckhuysen, Space- and time-resolved in-situ spectroscopy on the coke formation in molecular sieves: methanol-to-olefin conversion over H-ZSM-5 and H-SAPO-34, Chem. Eur. J. 14 (2008) 11320–11327.